

# Growth and Transformation Mechanism of Ternary CuAgSe Dendrites from Binary Ag<sub>2</sub>Se Dendrites

Yuanhao Gao,<sup>\*,[a]</sup> Zhi Zheng,<sup>[a]</sup> Yupeng Tian,<sup>[b]</sup> Yidong Zhang,<sup>[a]</sup> and Yange Zhang<sup>[a]</sup>

**Keywords:** Dendrimers / Nanoparticles / Copper / Silver / Selenium / Synthetic methods / Template synthesis

For the first time, ternary CuAgSe dendrites on a Ag foil substrate have been synthesized at room temperature by inheriting the dendritic structures of Ag<sub>2</sub>Se nanocrystals, and Cu nanoparticles and Se powders were used to feed the growth in aqueous ammonia solution. The new nano approach for the fabrication of CuAgSe dendrites can be re-

garded as a successful chemical alternative to the recently developed technique for electrochemical atomic layer epitaxy deposition for chalcogenides. The transformation process and mechanism from the binary Ag<sub>2</sub>Se phase to the ternary CuAgSe phase are discussed along with analysis their of thermodynamic, kinetic, and crystallographic properties.

## Introduction

In current nanomaterial studies, researchers have recognized that crystalline semiconductors with different morphologies exhibit different physical and chemical properties even if their chemical compositions are the same.<sup>[1,2]</sup> In some examples in electrochemical devices, 2D or 3D nanostructures or nanowires are more attractive than 1D nanorods or nanowires because they can transport holes or electrons more effectively through interconnected networks in the 2D and 3D scaffolds.<sup>[3]</sup> Nanodendrites are such network materials and their 3D dendritic nanostructures can provide both electrical links and a high surface/volume ratio. To date, some binary metal chalcogenide dendrites have been synthesized. For example, well defined hierarchical cadmium sulfide nanodendrites have been synthesized by hydrothermal treatment with CdCl<sub>2</sub> and thiourea as reagents and poly(ethyleneglycol) as a capping agent.<sup>[4]</sup> Recently, copper sulfide dendrites have been prepared in high yields by a concentration-controlled reaction of ethylenediamine and tributylphosphite.<sup>[5]</sup> We have previously demonstrated an in situ reaction strategy for the fabrication of both Ag<sub>2</sub>Se and Cu<sub>2-x</sub>Se dendrites.<sup>[6,7]</sup> Despite the considerable fabrication of binary metal chalcogenides with dendritic structures, to the best of our knowledge, ternary dendrite compounds have not been reported to date.

CuAgSe, an important ternary selenide, has some similar properties and applications to silver and copper selenides. For example, CuAgSe is a superionic conductor due to the mobility of both the Cu<sup>+</sup> and Ag<sup>+</sup> ions, and can be used in

electrochemical devices.<sup>[8–10]</sup> However, unlike most of the silver and copper selenides, CuAgSe is rarely studied due to the difficulty of its synthesis. The synthesis of ternary chalcogenides, including CuAgSe, from an aqueous solution of the component elements by hydrazine reduction has been proven by Kulify.<sup>[11]</sup> CuAgSe can be thermochemically prepared by heating a mixture of Ag, Cu, and Se to over 1000 K, with several heating and cooling processes.<sup>[12,13]</sup> The present interest in the synthesis of CuAgSe has been provoked by the report that a CuAgSe polycrystalline membrane has been commercialized for Cu<sup>2+</sup> ion-selective electrodes with a lifetime as long as ten years.<sup>[14]</sup> Recently, CuAgSe films have been electrochemically synthesized by a technique for electrochemical atomic layer epitaxy deposition for chalcogenides<sup>[15,16]</sup> first proposed by Stickney.<sup>[17]</sup>

In this paper, we report the design of a new nano approach to grow ternary CuAgSe dendrites at room temperature by inheriting the initial dendritic structures of Ag<sub>2</sub>Se reagents, and Cu nanoparticles and Se powders are used to feed the growth in aqueous ammonia solution. The reaction design adopts the electrochemical behavior studied by Neshkova et al.<sup>[15]</sup> that the ternary CuAgSe phase appears at potentials close to or coincident with those that lead to the deposition of binary compounds, Ag<sub>2</sub>Se and Cu<sub>2</sub>Se. Thus, it is believed that both Ag<sub>2</sub>Se and Cu<sub>2</sub>Se are prerequisites for CuAgSe growth at room temperature. The design further adopts the behavior of Cu<sub>2</sub>Se formation when elemental Se and Cu are in contact.<sup>[18]</sup> The two design concepts led to our new nano approach using Cu nanoparticles and Se powders for the growth of dendritic CuAgSe nanocrystals by inheriting the initial dendritic structures of the Ag<sub>2</sub>Se reagents. In this work, the dendritic Ag<sub>2</sub>Se reagents were prepared on Ag foil substrate (Ag<sub>2</sub>Se/Ag) so that the as synthesized CuAgSe dendrites on Ag foil substrate (CuAgSe/Ag) can be easily separated from the unreacted Cu nanoparticles and Se powders. The resulting CuAgSe den-

[a] Institute of Surface Micro and Nano Materials, Xuchang University, Xuchang 461000, China  
Fax: +86-374-4369210  
E-mail: gyh-2007@sohu.com

[b] Department of Chemistry, Anhui University, Hefei 230039, China

drites display highly symmetric corollitic morphology, similar to that of the initial  $\text{Ag}_2\text{Se}$  template reagents. This paper describes the transformation process and mechanism from dendritic  $\text{Ag}_2\text{Se}$  nanocrystals to crystalline  $\text{CuAgSe}$  dendrites. The new nano approach for the fabrication of  $\text{CuAgSe}$  can be regarded as a successful chemical alternative to the electrochemical atomic layer epitaxy deposition technique for chalcogenides, and could be applied to the fabrication of other ternary semiconductors with specific, desirable morphology.

## Results and Discussion

### The Synthesis and Characterization of $\text{CuAgSe}$ Dendrites

Ternary  $\text{CuAgSe}$  dendrites on a Ag foil substrate ( $\text{CuAgSe}/\text{Ag}$ ) were fabricated by inheriting the dendritic structure of  $\text{Ag}_2\text{Se}$  nanocrystals on a Ag foil substrate ( $\text{Ag}_2\text{Se}/\text{Ag}$ ). The reaction design adopts the electrochemical behavior of the admixture of  $\text{Cu}_2\text{Se}$  and  $\text{Ag}_2\text{Se}$  that immediately transforms structurally into the ternary  $\text{CuAgSe}$  phase at room temperature.<sup>[15]</sup> In our experiment, the dendritic  $\text{Ag}_2\text{Se}/\text{Ag}$  was first immersed in a Se powder suspension in water to adsorb Se powders on the surface of  $\text{Ag}_2\text{Se}$  dendrites ( $\text{Se}-\text{Ag}_2\text{Se}/\text{Ag}$ ). In the second step, the  $\text{Se}-\text{Ag}_2\text{Se}/\text{Ag}$  foil was immersed in a freshly prepared Cu nanoparticle suspension in an aqueous ammonia solution. In the two stage process, the residual Se powders on the surface of the  $\text{Ag}_2\text{Se}$  dendrites were treated with the freshly prepared Cu nanoparticles to form residual  $\text{Cu}_2\text{Se}$  on the surface of the  $\text{Ag}_2\text{Se}$  dendrites ( $\text{Cu}_2\text{Se}-\text{Ag}_2\text{Se}/\text{Ag}$ ). As growth proceeds, the dendritic  $\text{Ag}_2\text{Se}$  reagents reacted with the residual  $\text{Cu}_2\text{Se}$  to form  $\text{CuAgSe}$  dendrites at room temperature. It is worth noting that the Ag substrate in the dendritic  $\text{Ag}_2\text{Se}/\text{Ag}$  reagent is a necessary element to separate the products from the suspension of Se powder and Cu nanoparticles in the two stage process.

Figure 1 shows the SEM morphologies of the dendritic  $\text{Ag}_2\text{Se}$  reagents and the as obtained  $\text{CuAgSe}$  dendrites. As shown in Figure 1 (a), the  $\text{Ag}_2\text{Se}$  dendrites display highly symmetrical, hierarchical, corollitic morphology with a branch diameter of about 700 nm. After the conversion process, the  $\text{CuAgSe}$  products keep the well defined dendritic morphology, in which the dimensions, including diameter and thickness, are similar to those of the initial  $\text{Ag}_2\text{Se}$  template reagents (Figure 1, b).

XRD patterns of the dendritic  $\text{Ag}_2\text{Se}/\text{Ag}$  reagents and the dendritic  $\text{CuAgSe}/\text{Ag}$  product are shown in Figure 2. Figure 2 (a) shows the representative diffraction pattern of dendritic  $\text{Ag}_2\text{Se}/\text{Ag}$ , indicating that the  $\text{Ag}_2\text{Se}$  dendrite is in the orthorhombic  $\text{Ag}_2\text{Se}$  phase with cell constants of  $a = 4.333 \text{ \AA}$ ,  $b = 7.062 \text{ \AA}$ ,  $c = 7.764 \text{ \AA}$ , and  $Z = 4$  (JCPDS card, no. 24-1041), which we have discussed previously.<sup>[6]</sup> Figure 2 (b) shows the XRD pattern of dendritic  $\text{CuAgSe}/\text{Ag}$ . The diffraction peaks at  $2\theta = 28.30, 30.99, 34.20, 36.18, 42.46, 43.20, 44.18, 44.51, 48.80, 51.99, 53.60, 58.30$ , and  $63.32^\circ$  can be indexed to the (002), (110), (111), (012), (112), (003), (200), (020), (103), (211), (113), (212), and (203) planes of

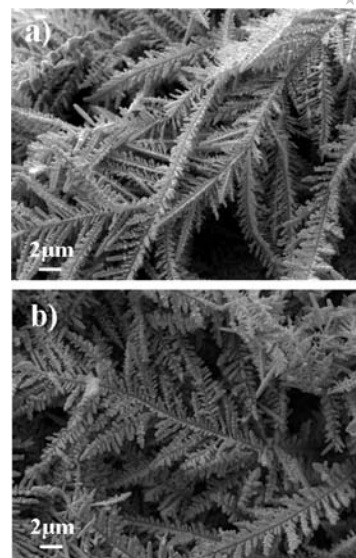


Figure 1. SEM morphologies of (a) dendritic  $\text{Ag}_2\text{Se}$  reagents; (b) as prepared  $\text{CuAgSe}$  dendrites.

orthorhombic  $\text{CuAgSe}$ , and the cell constants are calculated to be  $a = 4.112 \text{ \AA}$ ,  $b = 4.082 \text{ \AA}$ ,  $c = 6.322 \text{ \AA}$ , and  $Z = 2$ , which agree well with literature data (JCPDS card, no. 25-1180). In these XRD patterns, the diffraction peaks labeled with  $\clubsuit$  originate from the Ag substrate (JCPDS card, no. 87-720) as the dendrites are all present on a Ag foil substrate.

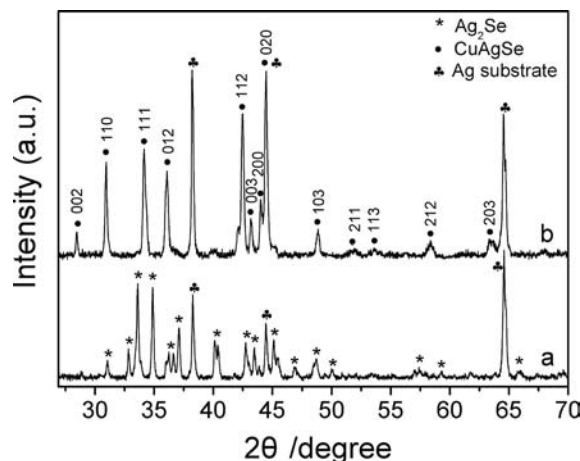


Figure 2. XRD patterns of (a) dendritic  $\text{Ag}_2\text{Se}$  reagents; (b) as prepared  $\text{CuAgSe}$  dendrites. All samples were present on the Ag foil substrate.

The as obtained  $\text{CuAgSe}$  dendrites were further studied by TEM. A representative TEM image of an individual dendrite branch is shown in Figure 3 (a). In this image, the diameter of the dendrite branch is about 700 nm. The selected-area electron diffraction (SAED) pattern shown in Figure 3 (b) shows the crystallinity of the dendrite branch and further confirms the nature of the single crystal. The SAED pattern can be indexed to the diffraction spots of orthorhombic  $\text{CuAgSe}$ . The stoichiometry of  $\text{CuAgSe}$  dendrite is 1.02:0.99:1.00 for the ratio of Cu:Ag:Se from energy

dispersive X-ray spectroscopy (EDX) data recorded from the boxed area in Figure 3 (a). We did not observe any other crystal phases of CuAgSe with TEM or XRD, indicating that the orthorhombic CuAgSe phase is the most common crystal phase at room temperature.

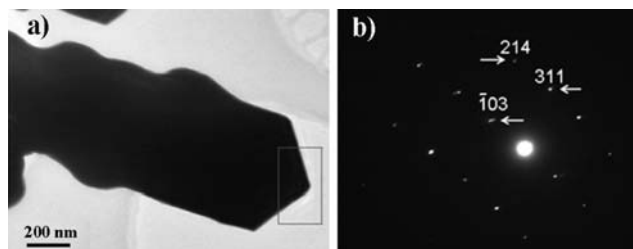
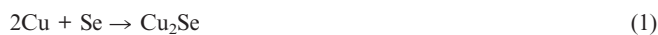


Figure 3. Representative TEM image of (a) an individual dendrite branch of CuAgSe dendrites and (b) the corresponding SAED pattern recorded from the boxed area in (a).

### Transformation Process from Binary Ag<sub>2</sub>Se Dendrites to the Target CuAgSe Dendrites

Zhang and coworkers have proven that Cu nanoparticles and Se powders with a Cu:Se molar ratio of 1:>2.5 can react to form binary Cu<sub>2</sub>Se nanoparticles in aqueous ammonia solution at room temperature.<sup>[18]</sup> A detailed electrochemical study of CuAgSe electrodeposition by Neshkova revealed that the admixture of Cu<sub>2</sub>Se and Ag<sub>2</sub>Se can immediately transform structurally into the ternary CuAgSe phase obeying a 1:1:1 molar ratio at room temperature.<sup>[15]</sup> Therefore, the transformation process from the Ag<sub>2</sub>Se phase to the CuAgSe phase can start with the following reaction; see Equations (1) and (2).



In our experiments, a trace amount of Se powder and an excess of Cu nanoparticles were used to ensure the formation of the pure Cu<sub>2</sub>Se phase on the surface of the dendritic Ag<sub>2</sub>Se reagents. Consequently, the binary Ag<sub>2</sub>Se phase transformed structurally into the target CuAgSe ternary phase by reacting with the pristine Cu<sub>2</sub>Se.

The powder XRD patterns in Figure 4 demonstrate the transformation process from the Ag<sub>2</sub>Se phase to the CuAgSe phase. Initially, only the orthorhombic Ag<sub>2</sub>Se reagents contribute to the patterns, except for some diffraction peaks originating from the Ag substrate (Figure 4, a). After repeating the two stage process three times, a mixture of the orthorhombic Ag<sub>2</sub>Se reagents and the orthorhombic CuAgSe products is formed (Figure 4, b). Repeating the two stage process six times leads to the domination of CuAgSe over Ag<sub>2</sub>Se (Figure 4, c). After repeating the two stage process ten times, only diffraction peaks of the orthorhombic CuAgSe phase were observed, except for the diffraction peaks of the Ag substrate (Figure 4, d), which indicates the total transformation of the orthorhombic Ag<sub>2</sub>Se phase into the orthorhombic CuAgSe phase. On the whole, no unre-

acted Cu<sub>2</sub>Se phase was observed in these XRD patterns. In fact, the unreacted Cu<sub>2</sub>Se phase was found in the final Cu nanoparticle suspension, and proved to be the monoclinic Cu<sub>2</sub>Se phase with cell constants  $a = 14.087 \text{ \AA}$ ,  $b = 20.481 \text{ \AA}$ ,  $c = 4.145 \text{ \AA}$ ,  $\beta = 90.38^\circ$ , and  $Z = 24$  (Figure 5).

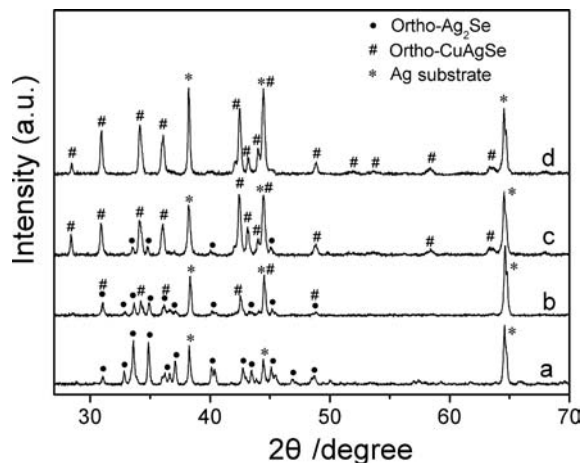


Figure 4. XRD patterns of (a) dendritic Ag<sub>2</sub>Se reagents; the reaction mixture obtained from the two stage process repeated (b) three times and (c) six times; (d) the as prepared CuAgSe dendrites obtained from the two stage process repeated ten times. All the samples are present on the Ag foil substrate.

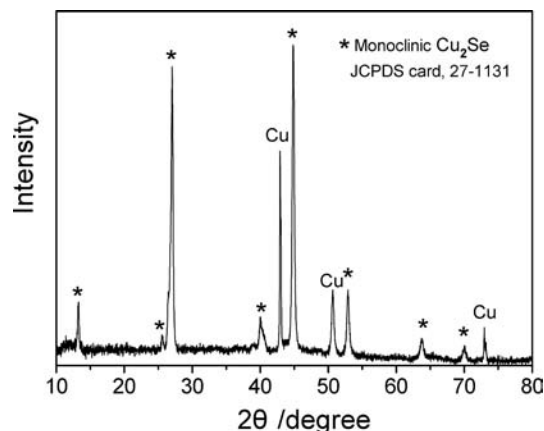


Figure 5. XRD patterns of the monoclinic phase of Cu<sub>2</sub>Se obtained from the final Cu nanoparticle suspension.

In order to explore the factors affecting the growth of dendritic CuAgSe nanocrystals, several control experiments at different concentrations of Se powders were performed and revealed a few interesting morphology changes as shown in Figure 6. Typically, the well defined dendritic CuAgSe nanocrystals were prepared by the two stage process repeated ten times with a Se concentration of 100 mg L<sup>-1</sup>. When the Se concentration was increased to 200 mg L<sup>-1</sup>, the pure CuAgSe dendrites were obtained by the two stage process repeated six times, however, a few CuAgSe agglomerates occurred (Figure 6, a). Further increasing the Se concentration to 500 or 700 mg L<sup>-1</sup>, repeating the two stage process three or four times led to pure CuAgSe products with rough dendritic branches (Figure 6, b and c). If the Se concentration was increased to 1.0 g L<sup>-1</sup>, repeating the two



stage process twice led to pure CuAgSe products in which the dendritic morphology was destroyed (Figure 6, d). From these results, it can be concluded that the rate of formation of the Cu<sub>2</sub>Se precursor plays an important role on the fabrication of the CuAgSe dendrites, which can be explained as follows: with a low Se concentration, which is a key factor in inheriting the initial dendritic structures, the dendritic Ag<sub>2</sub>Se/Se reagents obtained in first step have little residual Se that would be transformed into Cu<sub>2</sub>Se in the second step. Therefore, the rate of growth of the CuAgSe is limited due to the small amount of Cu<sub>2</sub>Se used to feed the growth. With the appropriate Se concentration and treatment with the two stage process, well defined dendritic CuAgSe crystals were obtained (see Figure 1, b).

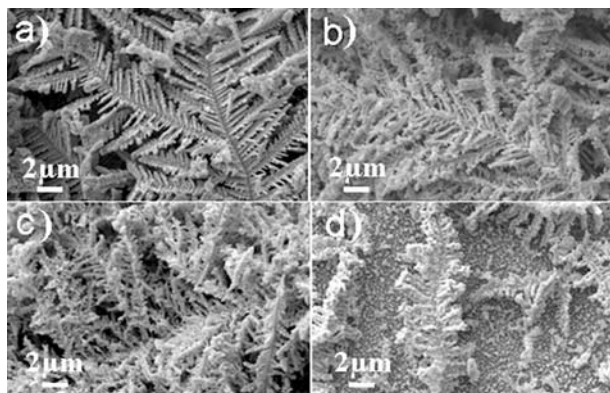


Figure 6. SEM morphologies of the as obtained CuAgSe products of (a) the two stage process repeated six times at a Se concentration of 200 mg L<sup>-1</sup>; (b) the two stage process repeated four times at a Se concentration of 500 mg L<sup>-1</sup>; (c) the two stage process repeated three times at a Se concentration of 700 mg L<sup>-1</sup>; (d) the two stage process repeated twice at a Se concentration of 1.0 g L<sup>-1</sup>.

### Transformation Mechanism from the Ag<sub>2</sub>Se Phase to the CuAgSe Phase

To probe into the formation mechanism from the Ag<sub>2</sub>Se phase to the CuAgSe phase, several control experiments were designed and performed in the same solvent system at room temperature by selecting different reaction precursors.

As above, the orthorhombic CuAgSe phase was prepared by reacting Ag<sub>2</sub>Se/Se composite with fresh Cu nanoparticles. Conversely, the orthorhombic CuAgSe phase was also obtained by reacting the Cu<sub>2</sub>Se/Se composite with fresh Ag nanoparticles. However, no CuAgSe phase was produced if the pure orthorhombic Ag<sub>2</sub>Se was used to react with fresh Cu nanoparticles or Cu<sup>2+</sup> ions (such as CuSO<sub>4</sub>). This suggests that Ag<sup>+</sup> ions in Ag<sub>2</sub>Se phase cannot be replaced by elemental Cu or Cu<sup>2+</sup> ions. Moreover, when the orthorhombic Ag<sub>2</sub>Se phase was mixed with a hexagonal CuSe phase or a tetragonal Cu<sub>3</sub>Se<sub>2</sub><sup>[18]</sup> no reaction occurred. Interestingly, if the pure orthorhombic Ag<sub>2</sub>Se reacted with Cu<sup>+</sup> ions (such as CuCl) in the aqueous ammonia solution, pure orthorhombic Cu<sub>0.5</sub>Ag<sub>1.5</sub>Se was obtained (Figure 7), which indicates that Ag<sup>+</sup> ions in the Ag<sub>2</sub>Se phase can be partially replaced only by Cu<sup>+</sup> ions at room temperature.

Significantly, when the orthorhombic Ag<sub>2</sub>Se was used to react with the monoclinic Cu<sub>2</sub>Se in aqueous ammonia solution, the orthorhombic CuAgSe phase was produced. This result supports the electrochemical behavior described by Neshkova<sup>[15]</sup> and indicates that both the monoclinic Cu<sub>2</sub>Se phase and orthorhombic Ag<sub>2</sub>Se phase can be adopted for the growth of the orthorhombic CuAgSe phase.

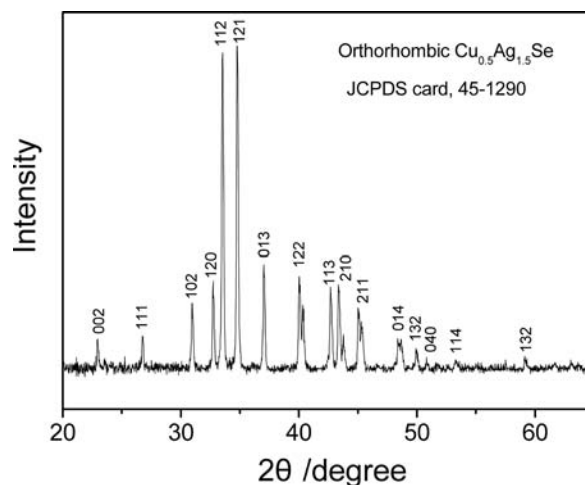
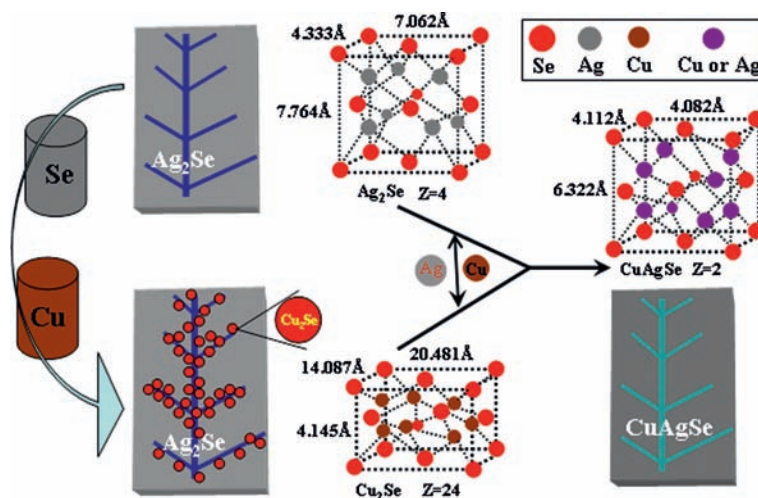


Figure 7. XRD pattern of the pure orthorhombic Cu<sub>0.5</sub>Ag<sub>1.5</sub>Se obtained by reacting Ag<sub>2</sub>Se with CuCl in aqueous ammonia solution.

From a structural perspective, it is worth noting that ternary CuAgSe can be represented formally as 1/2[Ag<sub>2</sub>Se]·1/2[Cu<sub>2</sub>Se]. Hence, formation of the CuAgSe phase is believed to relate to the assimilation between the monoclinic Cu<sub>2</sub>Se phase and the orthorhombic Ag<sub>2</sub>Se phase. Crystallographically, the crystal systems of the reactants (Ag<sub>2</sub>Se and Cu<sub>2</sub>Se) and the product (CuAgSe) are all alike, namely, an orthorhombic phase for Ag<sub>2</sub>Se and CuAgSe and a monoclinic phase for Cu<sub>2</sub>Se with only  $\beta = 90.38^\circ$  near to 90°, which is beneficial for the structural translation from the Ag<sub>2</sub>Se/Cu<sub>2</sub>Se phases to the CuAgSe phase. In fact, the structural translation from the Ag<sub>2</sub>Se/Cu<sub>2</sub>Se phases to the CuAgSe phase is only related to the slight variation at the bond angle and bond lengths of Cu–Se and Ag–Se. Thermodynamically, the structural translation process from the Ag<sub>2</sub>Se/Cu<sub>2</sub>Se phases to the CuAgSe phase can take place spontaneously according to the calculated  $\Delta G_{(298)}$  (–35.5 kJ mol<sup>-1</sup>), which is calculated as follows: consulting the literature,<sup>[15,19]</sup> the Gibbs free energies  $G_{(298)}$  for Ag<sub>2</sub>Se, Cu<sub>2</sub>Se, and CuAgSe are –49.4, –73.4, and –96.9 kJ mol<sup>-1</sup>, respectively. Therefore, the free energy changes for the formation of CuAgSe are calculated to be  $\Delta G_{(298)} = -35.5 \text{ kJ mol}^{-1}$ , according to the equation  $0.5\text{Ag}_2\text{Se} + 0.5\text{Cu}_2\text{Se} \rightarrow \text{CuAgSe}$ .

We speculate that assimilation between the Cu<sub>2</sub>Se phase and the Ag<sub>2</sub>Se phase may be due to ion exchange between the Cu<sup>+</sup> and Ag<sup>+</sup> ions. It is well known that Ag<sub>2</sub>Se, Cu<sub>2</sub>Se, and CuAgSe are superionic conductors with a high mobility of Cu<sup>+</sup>/Ag<sup>+</sup> ions. Kinetically, cation exchange between Ag<sub>2</sub>Se and Cu<sub>2</sub>Se can easily take place due to the high mobility of Cu<sup>+</sup> and Ag<sup>+</sup> ions. The control experiment for the formation of Cu<sub>0.5</sub>Ag<sub>1.5</sub>Se provides some support



Scheme 1. The formation mechanism of the  $\text{Ag}_2\text{Se}$  phase to the  $\text{CuAgSe}$  phase. The unit cells with cell constants are placed beside the corresponding products.

for the cation exchange mechanism. On the basis of the experimental results and speculations, the formation mechanism from the  $\text{Ag}_2\text{Se}$  phase to the  $\text{CuAgSe}$  phase is illustrated in Scheme 1.

## Conclusions

In this paper, we demonstrate a new nano approach for the fabrication of ternary  $\text{CuAgSe}$  nanodendrites from dendritic  $\text{Ag}_2\text{Se}$  nanocrystals assisted by copper nanoparticles and selenium powder. The resulting  $\text{CuAgSe}$  dendrites display highly symmetric, corollitic morphology, which is similar to that of the initial  $\text{Ag}_2\text{Se}$  reagent, including diameter and thickness. We found that the monoclinic  $\text{Cu}_2\text{Se}$  could react with the orthorhombic  $\text{Ag}_2\text{Se}$  to form orthorhombic  $\text{CuAgSe}$  in ammonia solution at room temperature. These new findings can be regarded as a successful chemical alternative of the electrochemical atomic layer epitaxy deposition technique for preparing chalcogenides. It was found that low Se concentration is a key factor for inheriting the initial dendritic structure of  $\text{Ag}_2\text{Se}$  nanocrystals. This work demonstrates the availability of in situ template conversion routes in the field of duplicating nanostructures, especially for some particular morphologies. It is worth noting that the nanosized  $\text{CuAgSe}$  particles were also obtained in ammonia solution without any substrate using the new nano approach. We advocate the new nano approach as a practical method for the synthesis of  $\text{CuAgSe}$  nanoparticles, especially those with particular morphologies.

## Experimental Section

**General:** All the reagents are of analytical grade and were used in experiments without further purification.  $\text{Ag}_2\text{Se}$  dendrites on a Ag foil substrate ( $\text{Ag}_2\text{Se}/\text{Ag}$ ) were prepared as we described previously.<sup>[6]</sup> Typically, the synthesis of  $\text{CuAgSe}$  dendrites on a Ag foil substrate ( $\text{CuAgSe}/\text{Ag}$ ) was performed at room temperature as follows: in the first step, the dendritic  $\text{Ag}_2\text{Se}/\text{Ag}$  ( $2 \times 0.3$  cm,  $\text{Ag}_2\text{Se}$

thickness 0.05 mm) was immersed in a Se powder suspension in water (Se concentration:  $100 \text{ mg L}^{-1}$ ) for 5–10 min to adsorb the Se powders on the surface of the  $\text{Ag}_2\text{Se}$  dendrites ( $\text{Se}-\text{Ag}_2\text{Se}/\text{Ag}$ ). In the second step, the  $\text{Se}-\text{Ag}_2\text{Se}/\text{Ag}$  foil was immersed for 10–15 min in a suspension of Cu nanoparticles ( $0.1 \text{ mol L}^{-1}$ , 50 mL) in aqueous ammonia solution that had been freshly prepared as reported.<sup>[18]</sup> In this process, the residual Se powders on the surface of the  $\text{Ag}_2\text{Se}$  dendrites were treated with freshly prepared Cu nanoparticles to form residual  $\text{Cu}_2\text{Se}$  on the surface of the  $\text{Ag}_2\text{Se}$  dendrites ( $\text{Cu}_2\text{Se}-\text{Ag}_2\text{Se}/\text{Ag}$ ). As the growth proceeds, the freshly prepared  $\text{Cu}_2\text{Se}$  was treated with dendritic  $\text{Ag}_2\text{Se}$  reagents to form  $\text{CuAgSe}$  dendrites ( $\text{CuAgSe}/\text{Ag}$ ). The two stage process was repeated several times to deplete the  $\text{Ag}_2\text{Se}$  reagents. Finally, the  $\text{CuAgSe}$  dendrites on the Ag foil substrate ( $\text{CuAgSe}/\text{Ag}$ ) were obtained by washing the product several times with water.

X-ray diffraction (XRD) patterns were recorded with a Philips MPD 18801 diffractometer using  $\text{Cu-K}_\alpha$  radiation ( $\lambda = 1.54178 \text{ \AA}$ ). Scanning electron micrographs were taken using a JSM-5600 scanning electron microscope. TEM images and SAED patterns were obtained with a JEOL JEM 2100 high-resolution transmission electron microscope operated at 200 kV equipped with an Oxford INCA EDX, which was used to collect EDX data.

## Acknowledgments

This work was supported by the National Natural Science Foundation of China (NSFC) (grant number 20873118), the Program for New Century Excellent Talents in University (grant number NCET-08-0665), the Program for Science & Technology Innovation Talents in Universities of Henan Province (2011HASTIT029), the Innovation Scientists and Technicians Troop Construction Projects of Henan Province (grant number 104100510001, 094300510064), and the Henan Province Science and Technology Key Project (grant number 082102230036).

- [1] N. E. Kelly, S. O. Lee, K. D. M. Harris, *J. Am. Chem. Soc.* **2001**, *123*, 12682–12683.
- [2] J. Hulliger, *Angew. Chem.* **1994**, *106*, 151; *Angew. Chem. Int. Ed. Engl.* **1994**, *33*, 143–162.
- [3] I. Gur, N. A. Fromer, C. P. Chen, A. G. Kanaras, A. P. Alivisatos, *Nano Lett.* **2007**, *7*, 409–414.

- [4] Q. Q. Wang, G. Xu, G. R. Han, *Cryst. Growth Des.* **2006**, *6*, 1776–1780.
- [5] W. P. Lim, H. Y. Low, W. S. Chin, *Cryst. Growth Des.* **2007**, *7*, 2429–2435.
- [6] D. P. Li, Z. Zheng, Z. Y. Shui, M. Q. Long, J. Yu, K. W. Wong, L. Yang, L. Z. Zhang, W. M. Lau, *J. Phys. Chem. C* **2008**, *112*, 2845–2850.
- [7] D. P. Li, Z. Zheng, Y. Lei, S. X. Ge, Y. D. Zhang, Y. G. Zhang, K. W. Wong, F. L. Yang, W. M. Lau, *CrystEngComm* **2010**, *12*, 1856–1861.
- [8] R. A. Yakshibaev, M. K. Balapanov, N. N. Mukhamadeeva, G. R. Akmanova, *Phys. Status Solidi A* **1989**, *112*, 97–100.
- [9] P. Pasierb, R. Gajerski, S. Komornicki, M. Reogonkas, *J. Therm. Anal. Calorim.* **2004**, *77*, 105–110.
- [10] K. Basar, T. Shimoyama, D. Hosaka, L. Xiang, T. Sakuma, M. J. Arai, *J. Therm. Anal. Calorim.* **2005**, *81*, 507–510.
- [11] S. M. Kulifay, *J. Am. Chem. Soc.* **1961**, *83*, 4916–4919.
- [12] K. Chrissafis, N. Vouroutzis, K. M. Paraskevopoulos, N. Frangis, C. Manolikas, *J. Alloys Compd.* **2004**, *385*, 169–172.
- [13] R. B. Baikulov, Y. G. Asadov, *Inorg. Mater.* **2005**, *41*, 338–342.
- [14] M. Neshkova, E. Havas, *Anal. Lett.* **1983**, *16*, 1567–1580.
- [15] M. T. Neshkova, V. D. Nikolova, A. M. Bond, V. Petrov, *Electrochim. Acta* **2005**, *50*, 5606–5615.
- [16] M. T. Neshkova, V. D. Nikolova, V. Petrov, *Anal. Chim. Acta* **2006**, *573–574*, 34–40.
- [17] B. W. Gregory, J. L. Stickney, *J. Electroanal. Chem.* **1991**, *300*, 543–561.
- [18] S. Y. Zhang, C. X. Fang, Y. P. Tian, K. R. Zhu, B. K. Jin, Y. H. Shen, J. X. Yang, *Cryst. Growth Des.* **2006**, *12*, 2809–2813.

Received: April 24, 2011  
Published Online: August 5, 2011